Title
Endothelial FAK is essential for vascular network stability, cell survival, and lamellipodial formation

Permalink
https://escholarship.org/uc/item/5g738140

Authors
Braren, Rickmer
Hu, Huiqing
Kim, Yung Hae
et al.

Endothelial FAK is essential for vascular network stability, cell survival, and lamellipodial formation

Rickmer Braren,[1] Huiqing Hu,[1] Yung Hae Kim,[1] Hilary E. Beggs,[2,3] Louis F. Reichardt,[2] and Rong Wang[1]

[1]The Pacific Vascular Research Laboratory, Division of Vascular Surgery, Department of Surgery, [2]Program in Neuroscience, Department of Physiology, Howard Hughes Medical Institute, and [3]Department of Ophthalmology, University of California, San Francisco, San Francisco, CA 94143

Morphogenesis of a vascular network requires dynamic vessel growth and regression. To investigate the cellular mechanism underlying this process, we deleted focal adhesion kinase (FAK), a key signaling mediator, in endothelial cells (ECs) using Tie2-Cre mice. Targeted FAK depletion occurred efficiently early in development, where mutants exhibited a distinctive and irregular vasculature, resulting in hemorrhage and lethality between embryonic day (e) 10.5 and 11.5. Capillaries and intercapillary spaces in yolk sacs were dilated before any other detectable abnormalities at e9.5, and explants demonstrate that the defects resulted from the loss of FAK and not from organ failure. Time-lapse microscopy monitoring EC behavior during vascular formation in explants revealed no apparent decrease in proliferation or migration but revealed increases in cell retraction and death leading to reduced vessel growth and increased vessel regression. Consistent with this phenotype, ECs derived from mutant embryos exhibited aberrant lamellipodial extensions, altered actin cytoskeleton, and nonpolarized cell movement. This study reveals that FAK is crucial for vascular morphogenesis and the regulation of EC survival and morphology.

Introduction

Mouse vascular morphogenesis begins in the yolk sac (YS) on embryonic day (e) 6.5, when endothelial cells (ECs) differentiate from mesenchymal-derived precursors (angioblasts) in the blood islands of the extraembryonic mesoderm. ECs subsequently coalesce into a honeycomb-shaped primitive capillary plexus. This de novo formation of blood vessels is called vasculogenesis and occurs slightly later in the embryo proper. By e8.5, the dorsal aortae, cardinal veins, and the surrounding primitive vascular plexus emerge. To assemble a mature vascular network composed of a hierarchy of arteries, arterioles, capillaries, postcapillary venules, and veins, the primitive vasculature undergoes a profound remodeling starting at e8.5 involving vessel expansion and regression (Haar and Ackerman, 1971; Risau, 1997).

Angiogenesis, the growth of new capillaries from pre-existing blood vessels, plays an essential role in vascular expansion (Yancopoulos et al., 2000; Rossant and Howard, 2002; Carmeliet, 2003). Two mechanisms are involved in forming new vascular segments. Sprouting angiogenesis is the extension of new vessels from existing capillaries into avascular tissues. It is thought that tip cell migration results in a decrease in EC-to-cell contacts, triggering EC proliferation and generation of new blood vessels (Ausprunk and Folkman, 1977). Thus, EC migration and proliferation are crucial events in sprouting angiogenesis. Intussusceptive angiogenesis is a process in which new vessels are formed by the insertion and extension of translumenal tissue pillars. It is hypothesized that these processes require no immediate proliferation of ECs; rather, they depend on the rearrangement of existing cells through the regulation of cell migration and adhesion (Burri and Djonov, 2002).

Vascular regression, or pruning, is an essential remodeling process in which excess ECs or vascular segments are eliminated to construct an efficient network (Risau, 1997). It is believed that only a minority of blood vessels formed during embryonic development remain through adulthood (Risau and Flamme, 1995). The two most prominent examples of vascular regression are the primordial aortic arches and paired dorsal aortae, which exist only transiently in mammals (Moore and Persaud, 2003). The precise morphological events, along with the underlying cellular and molecular mechanisms, remain obscure.

Targeted mutagenesis of many signaling pathways (e.g., VEGF, angiopoietin, ephrinB2, Notch, or TGF-β) results in a defective primitive vascular network, suggesting that they are essential for vascular remodeling (Rossant and Howard, 2002). However, these signaling pathways often elicit an array of biological effects, and the precise cellular function and intracellular signaling events that mediate such function within ECs are unclear.

FAK is a ubiquitously expressed protein–tyrosine kinase that mediates integrin, growth factor, and mechanical stress signaling (Miranti and Brugge, 2002; Parsons, 2003; Schlaepfer et al., 2004). Localized to focal adhesions, it interacts with integrin-associated proteins, such as paxillin and talin, and elicits downstream signaling. Activation of FAK via tyrosine phosphorylation occurs when cells are grown on integrin ligands or are stimulated by certain growth factors. The importance of FAK in vascular morphogenesis is evident because of its abundant expression in the vasculature at the time of critical vascular development (Polte et al., 1994). Furthermore, *fak*-null embryos die at e8.5 with multiple defects, including a disorganized cardiovascular system (Ilic et al., 1995). The presence of ECs in $fak^{-/-}$ embryos indicates that the absence of *fak* does not prevent EC differentiation (Ilic et al., 2003). However, *fak*-null embryos fail to form vascular networks, suggesting that FAK functions in the subsequent angiogenesis and vascular remodeling.

In vitro experiments have also demonstrated that FAK relays angiogenic signaling from multiple pathways, including those of VEGF and angiopoietin-1, and mediates EC migration, survival, and proliferation (Abu-Ghazaleh et al., 2001; Kim et al., 2001; Maru et al., 2001; Qi and Claesson-Welsh, 2001; Orr and Murphy-Ullrich, 2004). It is well recognized that conclusions drawn from in vitro experiments can be inconsistent with in vivo findings. For example, in ECs as well as in other cell types, FAK is critical for in vitro cell proliferation (Gilmore and Romer, 1996; Zhao et al., 1998). However, no change in cell proliferation was detected in $fak^{-/-}$ embryos or in a brain-specific conditional deletion mutant (Ilic et al., 1995; Beggs et al., 2003), raising doubts about whether FAK is important for cell proliferation in vivo. Furthermore, studies in different cell types reveal differential effects of FAK on cell migration. For example, *fak*-null fibroblasts exhibit an increase in focal adhesion contacts and a decrease in cell migration (Ilic et al., 1995; Schlaepfer et al., 1999). However, HeLa cells expressing reduced levels of FAK by short inhibitory RNA demonstrate an increase in cell motility (Yano et al., 2004), raising the possibility that FAK may elicit diverse effects in different cell types. Thus, it is imperative to dissect FAK's role in specific cell lineages in an in vivo environment.

In this study, we selectively deleted *fak* in ECs during mouse embryogenesis and investigated the subsequent effects on vascular morphogenesis. We also monitored EC behavior using time-lapse microscopy of embryonic explants and isolated primary ECs. Our work, with its comprehensive in vivo and in vitro evidence, demonstrates that *fak* in ECs is required for vascular maintenance and that its deletion severely compromised EC survival and spreading, leading to vascular regression.
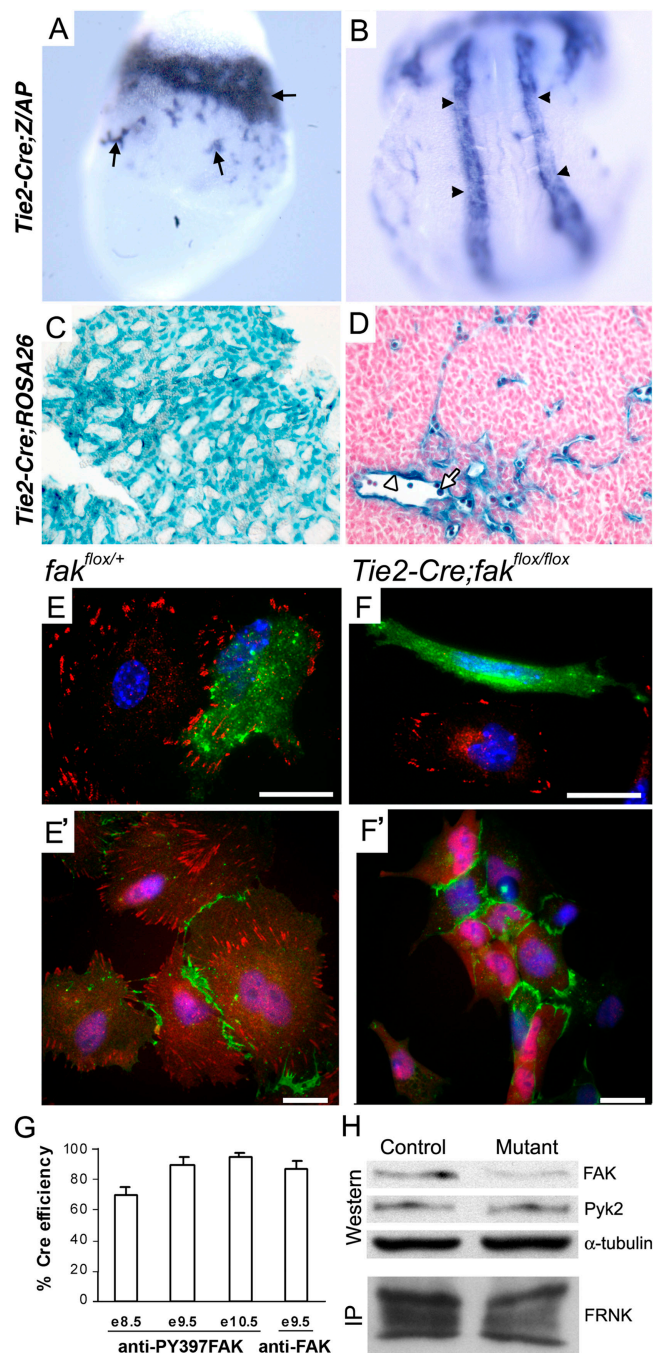

Figure 1. **Cre efficiently mediates gene excision early in the vasculature of *Tie2-Cre* embryos.** (A and B) AP-stained embryos at e7.5 (A) and e8.5 (B) show Cre activity in blood islands (arrows) and dorsal aortae (arrowheads). (C) A LacZ-stained YS at e11.5. (D) Paraffin section of e11.5 LacZ-stained embryo shows Cre activity in ECs (arrowhead) and blood cells (arrow). (E and F) FAK expression in cells from e9.5 embryos stained with anti-CD31 (green), DAPI (blue), and anti-Y397pFAK (red, E and F) or anti-FAK (red, E' and F'). Bars, 10 μm. (G) Cre-mediated FAK depletion was measured by the percentage of FAK$^-$ CD31$^+$ cells in mutants at e8.5, 9.5, and 10.5 relative to controls. Each represents the mean ± SEM (error bars) of 100 CD31$^+$ cells in three replicate (for anti-Y397FAK) and five replicate (for anti-FAK) experiments. (H) Expression of FAK, Pyk2, and FRNK by Western or IP analyses of e9.5 embryos.

Table I. **Depletion of *fak* in the vasculature results in hemorrhage and embryonic death at ~e11**

Embryonic stage	Litters	Number of embryos		Mutant embryos	
		Mutant/control	Bleeding	Alive	
e9.5	22	35/209 (17%)	0/35 (0%)	35/35 (100%)	
e10.5	15	28/141 (20%)	28/28 (100%)	22/28 (90%)	
e11.5	5	4/49 (8%)	NAª	0/4 (0%)	

ªNot applicable.

Results

Tie2-Cre efficiently mediates FAK depletion in early vascular development

To delete *fak* in ECs, we generated vascular-specific Cre mice using the *Tie2* promoter/enhancer (Schlaeger et al., 1997). To screen and characterize the mice, we used either Z/AP or Rosa26R reporter mice, in which AP or β-galactosidase activity, respectively, is activated only after Cre-mediated recombination (Lobe et al., 1999; Mao et al., 1999). From nine founder lines, we selected one that efficiently mediated gene excision. Cre was active at e7.5 in the blood islands of the extraembryonic mesoderm (Fig. 1 A), the earliest vascular cells, and in the dorsal aortae at e8.5 (Fig. 1 B). At e11.5, Cre was active in all vessels examined, including the vitelline vessels (Fig. 1 C). Histological evaluation revealed that Cre was active in ECs along with some blood cells (Fig. 1 D). These results demonstrated that Cre-mediated gene excision occurred specifically in early vascular progenitor cells, differentiated ECs, and some hematopoietic cells.

Using this Cre line, we created the conditional mutants (called mutants in this study) *Tie2-Cre; fak$^{flox/flox}$* and *Tie2-Cre; fak$^{flox/-}$*. Littermates missing any of the required alleles were used as controls throughout the study. In the *fak^{flox}* allele, two loxP sites flank the exon encoding the second kinase domain, which results in ablation of FAK protein expression but does not affect the expression of FAK-related nonkinase (FRNK; Beggs et al., 2003). To verify the excision of the *fak^{flox}* allele and the absence of FAK expression in ECs, we stained cells isolated from embryos because in situ identification of *fak*-null ECs was obscured by adjacent perivascular cells still expressing FAK. We performed double staining with anti–P-Y397FAK (Sieg et al., 2000) and anti-CD31 (an EC marker; Newman et al., 1990). FAK was present in the focal adhesion contacts of both CD31$^+$ and CD31$^-$ cells (Fig. 1 E). Although non-ECs from a mutant still expressed FAK, most CD31$^+$ cells from the mutant did not express FAK (Fig. 1 F). To assess the time course of the *Tie2-Cre*–mediated FAK depletion, we quantitatively analyzed endothelial FAK expression at different gestational stages. FAK was absent in ~70% of ECs at e8.5, ~90% at e9.5, and ~95% at e10.5 (Fig. 1 G). Thus, the *Tie2-Cre*–mediated deletion of *fak^{flox}* began before e8.5 and resulted in the nearly complete depletion of FAK protein in CD31$^+$ cells by e10.5.

To verify the loss of FAK expression, we performed double immunostaining with antibodies (Abs) specific to the COOH terminus of FAK and CD31 in purified ECs from e9.5 embryos and found similar FAK deletion (Fig. 1, E′–G). Furthermore, using this Ab, we examined lysates of e9.5 embryos by Western blotting. Despite the presence of other cell types, we detected a
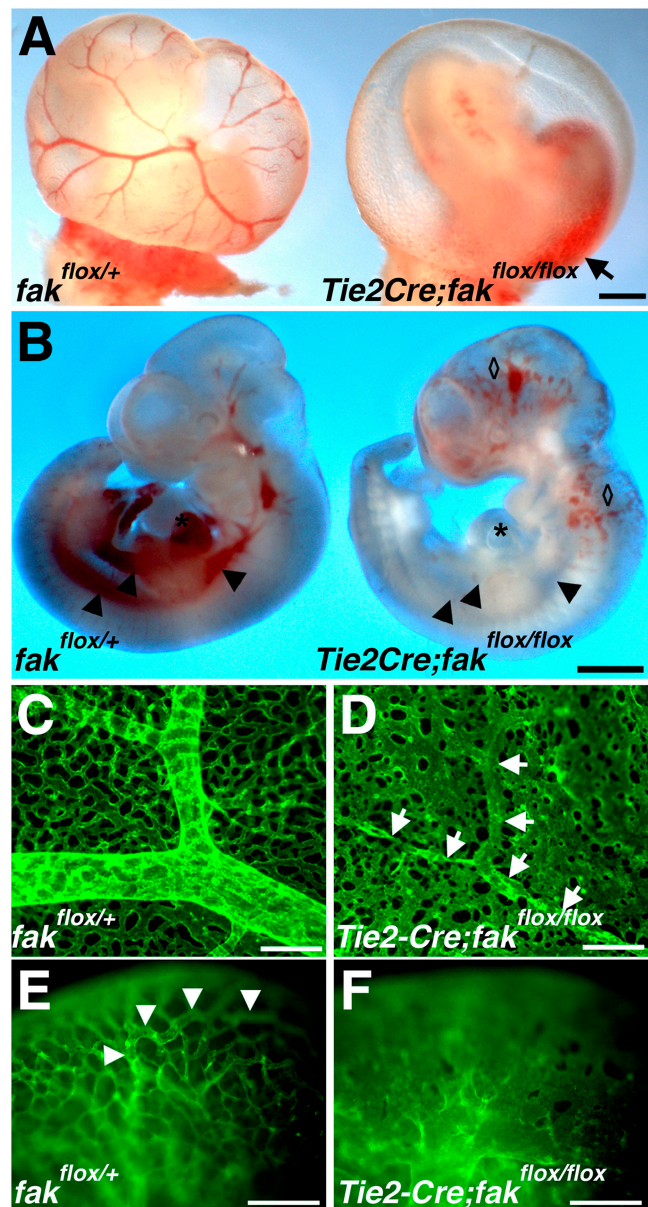

Figure 2. ***Tie2-Cre*–mediated FAK depletion causes hemorrhaging and vascular defects at e10.5.** (A and B) Images of freshly dissected YSs (A) and embryos (B). Arrow, bleeding; diamonds, dilated sinusoidal vessels; asterisk, heart; arrowheads, major vessels. Bars, 1 mm. (C and D) Micro-angiographs of CD31-stained YSs. Note that only the remnants of large vessels are identifiable in the mutant (D, arrows). (E and F) Microangiographs of CD31-stained heads. Arrowheads, internal carotid artery. Note the abnormally wide irregular vessels in the mutant. Bars, 200 μm.

significant reduction in FAK expression in the mutant (Fig. 1 H), further validating efficient *fak* deletion. Expression of FRNK was low, undetectable by Western blotting (unpublished data), and was unchanged by immunoprecipitation (IP; Fig. 1 H).

In contrast, the expression of Pyk2 (proline-rich tyrosine kinase 2), a FAK-related kinase, was unchanged in embryonic lysates (Fig. 1 H). We also performed triple immunostaining with Abs to CD31, FAK, and Pyk2 and found no obvious increase in Pyk2 signal in mutant ECs without FAK (Fig. S1, available at http://www.jcb.org/cgi/content/full/jcb.200506184/DC1).
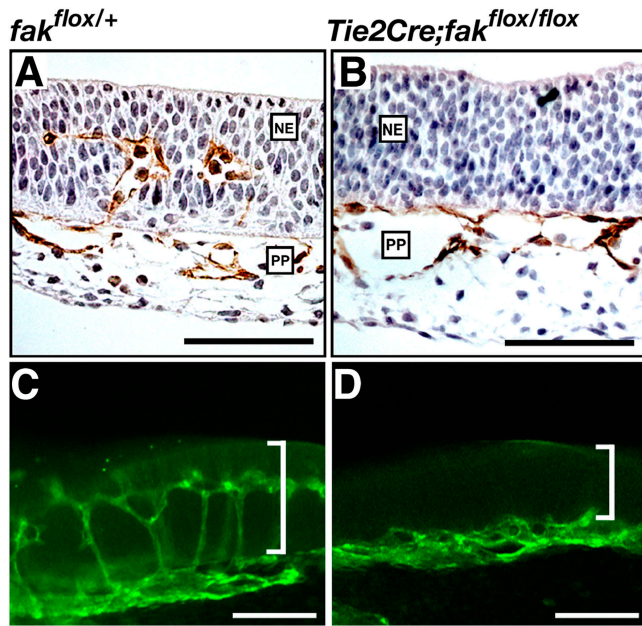
Figure 3. **Impaired sprouting angiogenesis into the NE in e10.5 mutants.** (A and B) Paraffin cross sections of the apical head stained for CD31 (brown). Note multiple small perineural plexus (PP) capillaries in the NE in the control (A) but not in the mutant NE (B). (C and D) 100-μm cross sections of the heads show the capillary network in the control NE (C) but not in the mutant (D). Brackets, width of the NE. Bars, 100 μm.

Deletion of *fak* disrupts the vasculature, leading to hemorrhage and death at e10.5–11.5

Because FAK is deleted in early development, we predicted that our mutants would die early in gestation from lethal vascular defects. However, at e9.5, no detectable gross abnormalities were observed (Table I and unpublished data). At e10.5, ∼10% of the mutants were dead, and the remaining live mutants were readily identified by severe vascular

defects. At e11.5, no live mutant embryos were recovered (Table I).

To determine the embryonic phenotype more precisely, we examined the mutant embryos at e10.5. The mutant YSs lacked the blood-filled vascular tree typically observed in the controls. Instead, hemorrhage was apparent in both the amniotic and YS cavities (Fig. 2 A). Although major structures were present in the embryo proper, the mutants were slightly smaller and showed patches of sequestered blood (reflecting dilated vessels) primarily in the upper trunk and head regions (Fig. 2 B).

To examine any endothelial abnormalities, we performed whole-mount immunostaining using anti-CD31 and found abundant CD31^{+} ECs organized in severely defective vascular structures. The mutant YSs lacked the hierarchical vitelline vascular pattern seen in the controls (Fig. 2 C), and only remnants of major vessels were observed (Fig. 2 D). The mutant capillary plexuses lacked the intricate network structure seen in the controls; instead, the microvessels were irregularly shaped, frequently dilated, and flattened with a sheetlike appearance and thin, spiky connections (Fig. 2 D and not depicted). We observed a distinct internal carotid artery that was well connected to a homogenous network of head capillary plexuses in the control (Fig. 2 E) but not in the mutants. Instead, as in the mutant YS, vessels appeared flat and fused to the surrounding widened and sinusoidal capillaries, leading to a great variation in the size of the capillaries and intercapillary spaces (Fig. 2 F).

Sprouting angiogenesis is absent in the neuroepithelium (NE)

Because the NE lacks mesenchymal cells, its vascularization is dependent entirely on the invasion of vessel branches generated from preexisting vessels in the surrounding tissues by sprouting angiogenesis (Kurz et al., 1996). We observed a complete absence of blood vessels in the NE at e10.5 by CD31 staining, indicating that the *fak*-null mutants were defective in sprouting angiogenesis into the NE (Fig. 3).
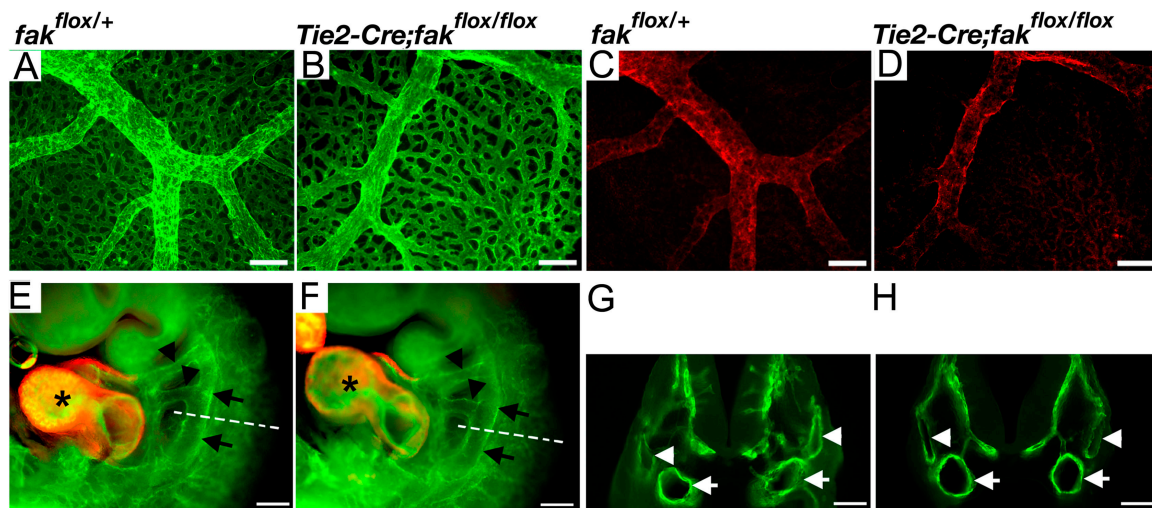

Figure 4. **e9.5 mutants display no gross defects in major vascular structures.** (A–D) Microangiographs of e9.5 YSs stained with Abs to CD31 (green, A and B) and SMαA (red, C and D). (E–H) Microangiographs of whole-mount (E and F) and thick-sectioned (G and H) embryos labeled with Abs to CD31 and SMαA. Arrows, dorsal aortae; black arrowheads, aortic arches; asterisks, heart chambers; white arrowheads, paired cardinal veins. Bars, 200 μm.

Vascular defects are the earliest detectable abnormalities

Because major vessels were severely defective at e10.5, we questioned whether they had never developed or had degenerated. To distinguish between these possibilities, we analyzed the vasculature at e9.5 by CD31 and smooth muscle α-actin (SMαA) double immunostaining. At e9.5, the mutant embryos were morphologically indistinguishable from the controls when viewed under a dissecting microscope (unpublished data). The appearance of mutant YS vasculature was surprisingly similar to that of controls, with comparable branching patterns and recruitment of smooth muscle cells, except that the vitelline arteries were slightly less elaborate (Fig. 4, A and B). Staining for SMαA revealed that smooth muscle cells were recruited to vitelline arteries in both the controls and mutants (Fig. 4, C and D).

In the e9.5 embryo proper, CD31 and SMαA double staining revealed no apparent differences between the head vasculature of the mutants and the controls (unpublished data). In addition, the major embryonic vessels (including the dorsal aortae, aortic arches, and cardinal veins) and cardiac chambers in the mutants had developed comparably (Fig. 4, E and F). To further verify these findings and to examine vessels that were not visible on the surface, we analyzed 100-μm–thick cross sections of CD31-stained embryos (Fig. 4, G and H), finding again that the dorsal aortae and cardinal veins were comparable. However, we noticed fewer small vessels in the mutant cross section (Fig. 4 H), suggesting that vascular defects had begun to develop.

Given that *Cre* is also expressed in hematopoietic cells in *Tie2-Cre* mice, we looked for defects in blood cells. Upon gross examination, blood was present in e9.5 mutant embryos and YSs, similar to the controls. Furthermore, we isolated e9.5 circulating hematopoietic cells and found no significant difference in the number of cells isolated from the controls and mutants (unpublished data). This result suggests that no obvious hematopoietic abnormalities had developed at this stage. Altogether, these phenotypic findings at e9.5 indicate that subtle vascular defects had begun to develop and that they are primary effects of the loss of FAK in ECs.

Dilated capillaries and intercapillary spaces are primary defects

To identify the cellular defects during vascular development, we focused on the highly reproducible irregular microvessel sizes seen in the e10.5 mutant YSs. To investigate this phenotype further and to avoid any secondary effects that might have contributed to it, we examined the mutants at e9.5, before other detectable abnormalities. High magnification microangiographs of mutant YSs showed wider capillary diameters, fewer small intercapillary spaces, and larger intercapillary areas that were often associated with incomplete vascular sprouts (Fig. 5, A and B). To confirm these observations quantitatively, we analyzed the YS microangiographs morphometrically. The mutant YSs had a 10-μm (25%) increase in mutant capillary width that was accompanied by a reduction in the number of intercapillary areas smaller than 200 μm^2 and an increased number of intercapillary spaces that were larger than
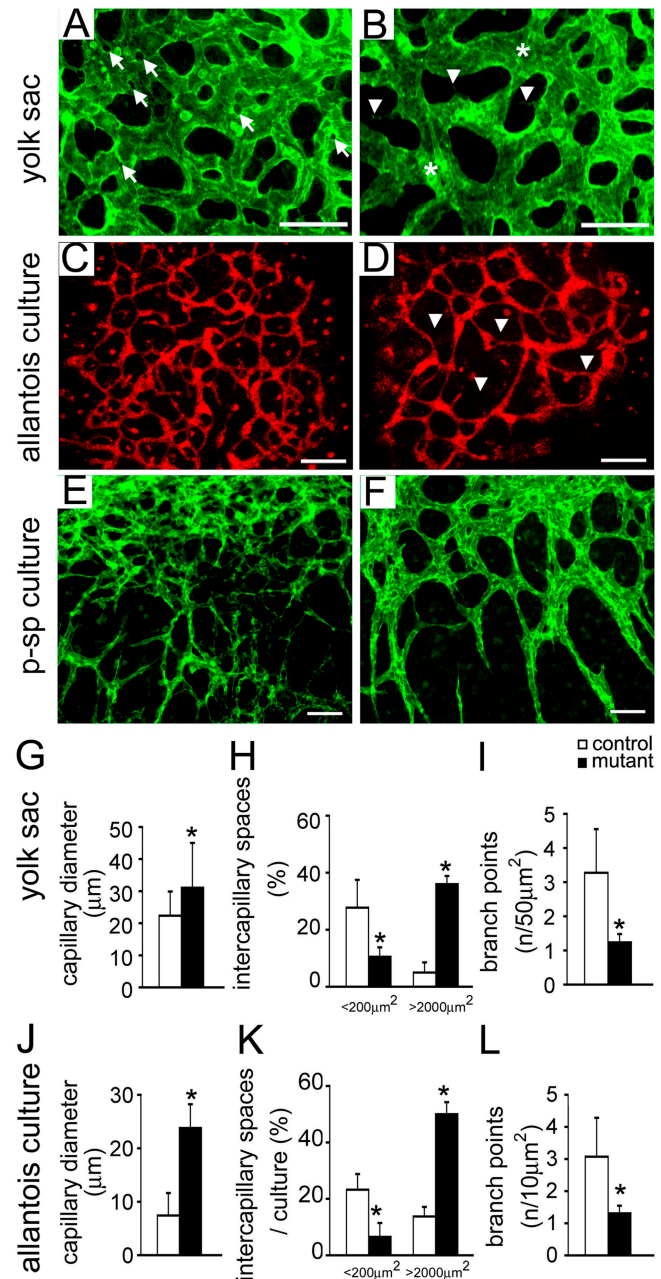

Figure 5. **Dilated capillaries and intercapillary spaces are primary defects.** (A and B) Microangiographs of e9.5 control (A) and mutant (B) YSs. Note fewer small intercapillary spaces (arrows), widened capillaries (asterisk), and more incomplete sprouts (arrowheads) in the mutant. Bars, 100 μm. (C and D) Microangiographs of control (C) and mutant (D) allantoic explants. Arrowheads, widened intercapillary spaces. Bars, 200 μm. (E and F) Microangiographs of control (E) and mutant (F) P-Sp explants. Note a reduction in network complexity and wider vessels in the mutants. (G–L) Quantification of capillary diameters, intercapillary space sizes, and number of branch points in YSs (G–I) and allantoic explants (J–L). Error bars represent SEM. *, P < 0.05.

2,000 μm^2 in diameter (Fig. 5, G and H). Branch points representing network complexity were significantly reduced in the mutants (Fig. 5 I).

To separate any influence of the heart, blood, or other organs that might contribute to the vascular phenotype, we analyzed capillary morphogenesis in embryonic explants ex vivo.
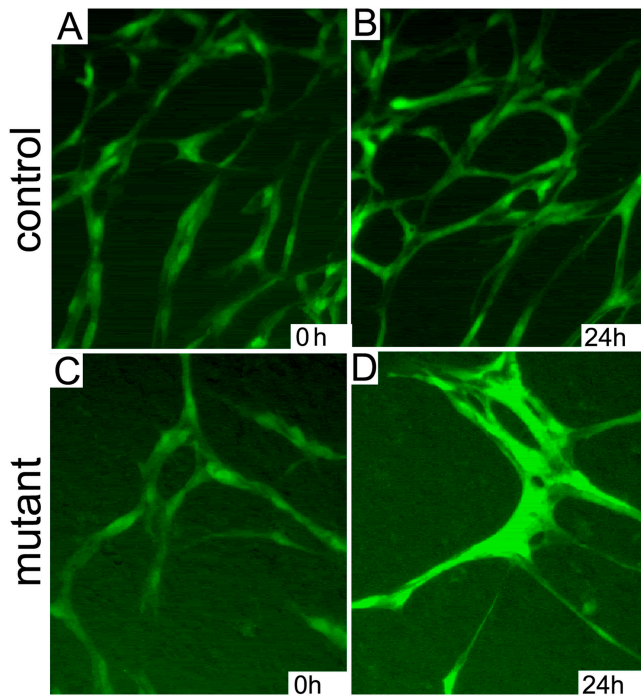
Figure 6. **Still images of capillaries in P-Sp explants.** Control (A) and mutant (C) explants show comparable capillary networks at 0 h, but at 24 h, there were fewer, wider vessels in the mutant (D) compared with the control (B).

Figure 7. **Increased death in FAK-deficient ECs.** (A) EC death in P-Sp explants as detected by time-lapse microscopy. (B) Cross sections of immuno-fluorescent stained e9.5 YSs. Red, CD31; green, TUNEL; arrowheads, TUNEL[+] ECs. Bars, 10 μm. (C) Apoptotic rate of ECs in the YSs. Bar graph represents the mean ± SEM (error bars) from three independent experiments. A total of 10,175 control and 7,878 mutant ECs were counted. *, $P < 0.05$. Control, white bars; mutant, black bars.

Microangiography of allantoic explants (Fig. 5, C and D) and para-aortic splanchnopleural mesoderm (P-Sp) explants (Fig. 5, E and F) revealed vascular phenotypes similar to those in the YSs. Dilation of capillaries and intercapillary spaces was observed along with a reduction in network complexity. A quantitative assessment revealed an approximate threefold increase in capillary width, which is a significant reduction in intercapillary spaces $<200 \ \mu m^2$, an increase in intercapillary spaces $>2,000 \ \mu m^2$, and a reduction in the number of branch points (Fig. 5, J–L). Because the explant phenotypes resembled the in vivo capillary defects, they likely represent the primary effects of *fak* deletion in ECs.

Table II. **Vascular morphogenesis in P-Sp explants**

Phenotype T_{start}[a] → $T_{observed}$	Frequency	
	Control[b] *n* (%)	Mutant *n* (%)
Sprout → growth[c]	58 (56.3)	40 (35.1)
Sprout → no change	14 (13.6)	15 (13.2)
Sprout → regression[d]	31 (30.1)	59 (51.8)
Subtotal	103 (100)	114 (100)
Network → growth[e]	39 (45.9)	22 (23.9)
Network → no change	30 (35.3)	23 (25.0)
Network → regression[d]	16 (18.8)	47 (51.1)
Subtotal	85 (100)	92 (100)

[a]The subcategories were defined as the phenotype at the initial point of time-lapse videos (T_{start}). The videos were captured at 10-min intervals for 24–48 h.
[b]Controls: *Tie2-Cre;fak^{flox/+}* or *fak^{flox/+}*; mutants: *Tie2-Cre;fak^{flox/flox}*.
[c]Elongation, widening, and network formation from sprouts.
[d]Reduction in length or size and degeneration, including cell death.
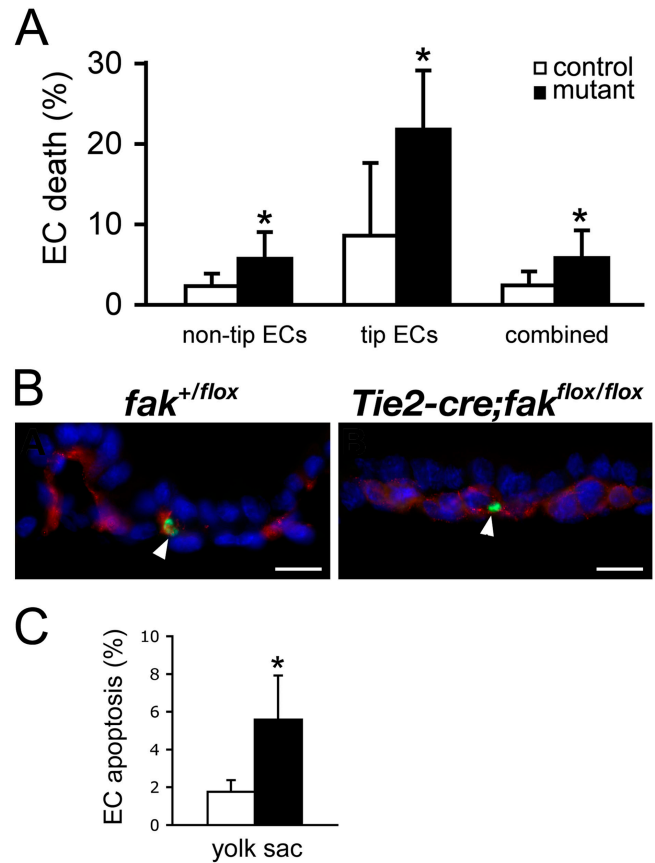[e]Increased network complexity and caliber.

Reduced vessel growth and increased vessel regression and contraction in mutant explants

To identify defects in vascular development, we performed time-lapse microscopy on P-Sp explants carrying an additional *Tie1-GFP* allele in which GFP is driven by an EC-specific promoter (Iljin et al., 2002). Because the P-Sp explants were taken from e8.5–9.5 embryos, most ECs had lost FAK. To ensure that Cre was active, we used the Rosa26R reporter and confirmed that explant vascular networks were positive for Cre activity (unpublished data). The most striking differences involved vessel contraction. The control explants (Fig. 6, A and B; and Video 1, available at http://www.jcb.org/cgi/content/full/jcb.200506184/DC1) retained a high level of network integrity. In contrast, the mutant explants (Fig. 6, C and D; and Video 2) underwent a process in which ECs contracted and clustered with each other, resulting in an irregular network composed of wider and smaller vessels, which is reminiscent of the e10.5 YS microvessels.

In addition, we analyzed endothelial sprouts and networks in 286 videos and found apparent vessel deterioration: 51.8% of mutant vessels regressed versus 30.1% of control sprouts, and 51.1% of mutant networks regressed versus 18.8%
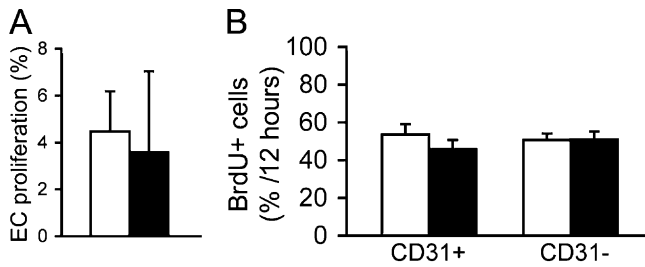
Figure 8. **Insignificant decrease in proliferation in FAK-deficient ECs.** (A) EC proliferation in P-Sp explants as measured by time-lapse microscopy. (B) EC proliferation measured by in vivo BrdU labeling. Each bar represents the mean ± SEM (error bars) of 100 cells in three independent experiments. Control, white bars; mutant, black bars.

of control networks (Table II). Furthermore, sprout and network growth was reduced in the mutants (35.1 vs. 56.3% and 23.9 vs. 45.9%, respectively; Table II). Together, these results suggest that ECs lacking FAK lead to reduced vessel growth and increased vessel regression.

FAK deletion in ECs results in increased death and no significant change in proliferation

To determine the cellular mechanism of the vascular defects, we analyzed cell survival, proliferation, and migration. We monitored 4,240 control and 3,895 mutant ECs in P-Sp explants over 8 h by time-lapse microscopy. The percentage of dying cells in the mutants was more than double that in controls (5.8 vs. 2.4%; Fig. 7 A). To examine whether there was a differential effect in sprout tip versus nontip cells, we monitored 78 control and 108 mutant tip cells. Again, the overall percentage of dying cells in the mutants was more than double that of controls (21.8 vs. 8.6%). To verify EC apoptosis in vivo,

we performed TUNEL along with CD31 staining on YS sections, which contain fewer cell types and allow for a clearer identification of ECs. We detected apoptotic ECs in both controls and mutants (Fig. 7 B), but quantitative analysis revealed a twofold increase in apoptotic ECs in the mutants (Fig. 7 C).

We did not detect any significant changes in EC proliferation in the explants (Fig. 8 A). To confirm this result, we quantified EC proliferation in vivo by injecting BrdU into pregnant mice. Cells were subsequently isolated from e9.5 embryos. The number of BrdU$^+$ CD31$^+$ cells was slightly, but insignificantly, reduced in the mutant, whereas the number of BrdU$^+$ CD31$^-$ cells remained the same (Fig. 8 B). Therefore, the loss of *fak* did not provoke significant change in EC proliferation but reduced EC survival, which is likely responsible for the reduced vascular growth and increased vascular regression.

No reduction in cell migration in FAK-null ECs

To investigate EC migration in the context of vessel morphogenesis, we examined ECs lining the vessels in P-Sp explants. We monitored the migration path of ECs over a 300-min period at 30-min intervals. From 13 control and 16 mutant ECs analyzed, six representative pairs are shown in Fig. 9 A, demonstrating no obvious difference. We quantified the velocity (distance/interval) of 33 control and 55 mutant ECs that were analyzed over a period of 8 h and found an average velocity of 10.7 ± 8.7 μm versus 12.2 ± 11.56 μm, respectively, indicating no major difference in the migration distance of mutant ECs within a vessel and a subtle, insignificant increase in velocity.

Because previous reports of cell migration of FAK-deficient cells were analyzed in isolated cells and not in an organ context (Ilic et al., 1995; Yano et al., 2004), we examined ECs that did not belong to a vessel structure but were scattered in the P-Sp explants. The migration paths of six representative pairs from
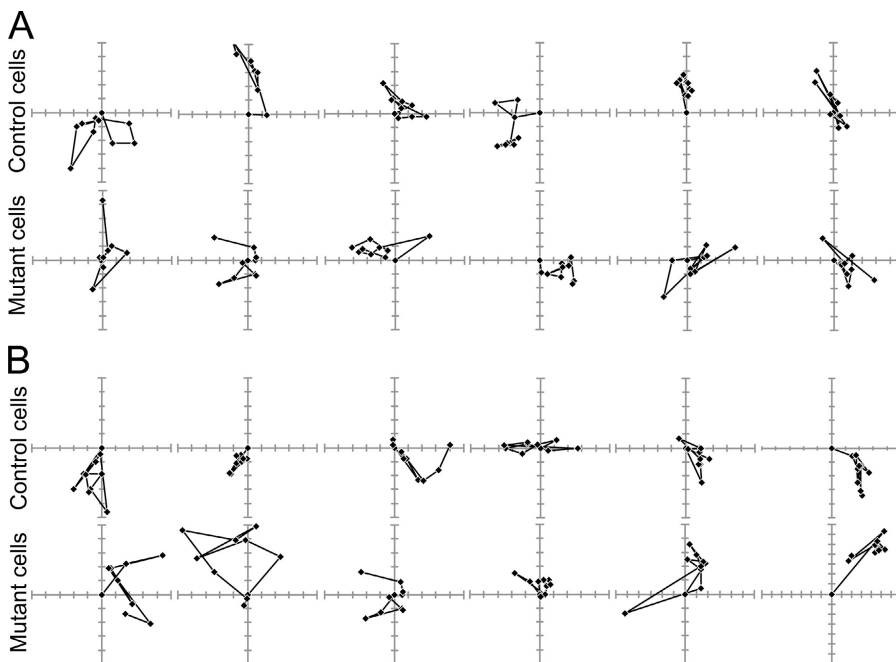

Figure 9. **Migration paths of individual FAK-deficient ECs in P-Sp explants.** Each point indicates the position (XY coordinates) of the cell at 30- (A, capillary ECs) or 28- (B, single ECs) min intervals. Positions of 10 consecutive intervals are shown. Each axis tick represents a distance of 10 μm.

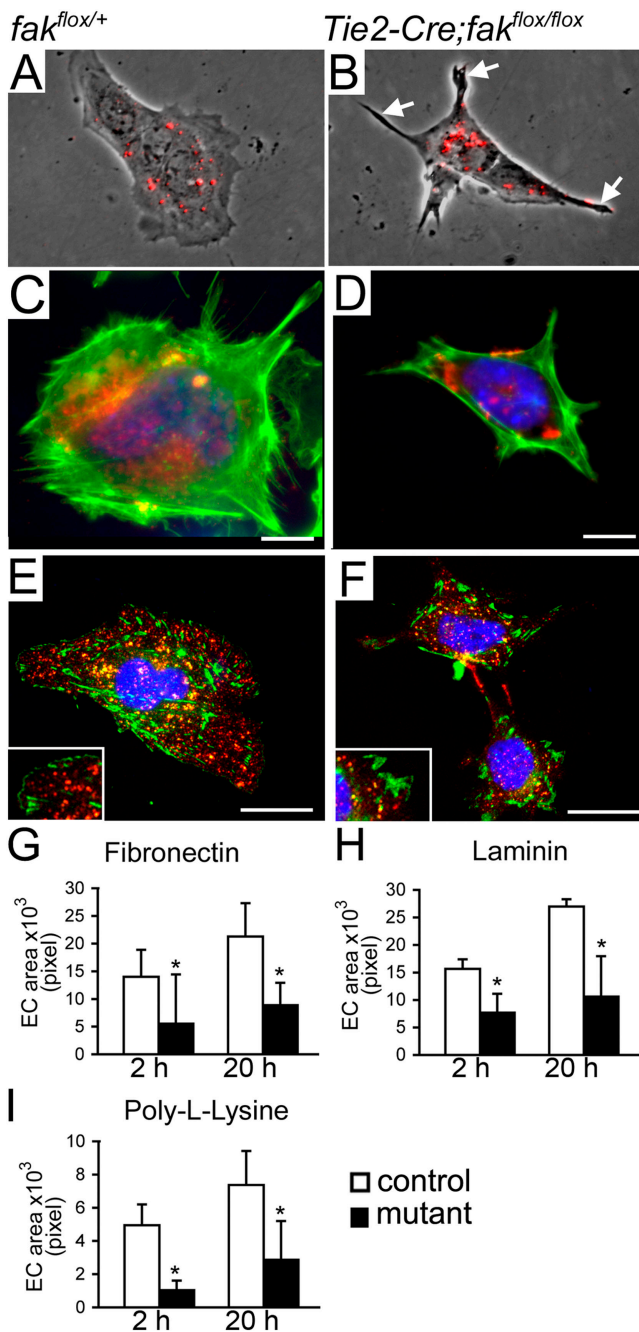
fak^flox/+
Tie2-Cre;fak^flox/flox
A
B
C
D
E
F
G
Fibronectin
H
Laminin
EC area x10^3 (pixel)
30
25
20
15
10
5
0
2 h
20 h
I
Poly-L-Lysine
10
8
6
4
2
*
□ control
■ mutant

Figure 10. **Mutant ECs display defective cell morphology and locomotion.** (A and B) Micrographs of ECs overlaid with DiI-Ac-LDL labeling (red). Mutant ECs display thin and spiky cell protrusions (arrows). (C–F) Immunofluorescent micrographs of actin organization (C and D) and focal adhesions (E and F) in ECs; insets, focal adhesions. Red, CD31; green, actin (C and D) or paxillin (E and F); blue, DAPI. Bars, 10 μm. (G–I) Time course of EC spreading on FN, LM, and PLL at 2 and 20 h. Each bar represents the ± SEM (error bars) of 50 cells examined in three replicate experiments. *, $P < 0.05$.

26 control and 34 mutant ECs analyzed at 28-min intervals over a 280-min period are shown in Fig. 9 B, demonstrating an increase in cell migration of the mutant ECs. Consistent with this result, the average velocity of 10 control and 15 mutant ECs analyzed over an 8-h period was 7.6 ± 6.6 μm versus 16.7 ± 12.8 μm, respectively.

We also monitored (at 10-min intervals over 8 h) the migration of isolated embryonic ECs, which were identified by DiI-Ac-LDL uptake or Tie1-GFP, grown on fibronectin (FN). Control ECs exhibited extensive membrane ruffling and lamellipodia formation at the migrating front (Fig. 10 A and Video 3, available at http://www.jcb.org/cgi/content/full/jcb.200506184/DC1). In contrast, mutant ECs were poorly spread and lacked membrane ruffling and lamellipodia formation (Fig. 10 B and Video 4). Spiky, thin cell protrusions extended at the cell periphery in a random fashion, compromising cell polarity. Neither the mutant nor the control clusters of ECs migrated a significant distance (unpublished data). The single mutant cells were actively moving, although they lacked the stable directional migration seen in the controls. To quantify cell migration, we tracked the cell center and found that single mutant ECs traveled ~50% longer distances compared with the controls (unpublished data). These results demonstrate that FAK-deficient single ECs exhibit a defective, but faster, locomotion on FN in the presence of serum and growth supplements.

FAK-null ECs displayed defective lamellipodia and cell spreading

To further identify the cellular defects resulting from FAK depletion in ECs, we examined the actin cytoskeletal structure. Phalloidin staining revealed typical actin stress fibers throughout the control ECs (Fig. 10 C). FAK-deficient ECs showed fewer and abnormal stress fibers that instead resembled cortical actin bundles (Fig. 10 D). Because *fak*$^{-/-}$ fibroblasts exhibit an increased number of focal adhesion contacts (Ilic et al., 1995), we stained our mutant ECs for paxillin, which is a component of focal adhesion contacts and an anchor for actin filaments. In contrast to the abundant, well-spread focal adhesions throughout the control cells, fewer focal adhesions that were peripherally confined (even aggregating together) were detected in the mutants (Fig. 10, E and F). These results suggest that the loss of *fak* leads to abnormal actin cytoskeleton structure and focal adhesion organization in ECs.

To determine the kinetics of cell spreading, we examined cells on FN and found a marked reduction in cell spreading at both 2 and 20 h after plating (Fig. 10 G). To ascertain whether this was a matrix-specific result, we plated cells on laminin (LM)-coated and poly-L-lysine (PLL)–coated plates and found similar defects in cell spreading (Fig. 10, H and I). Therefore, the loss of FAK compromised EC spreading through both ECM-dependent and independent mechanisms. In summary, these results suggest that the loss of *fak* leads to abnormal cell spreading without decreasing cell migration in ECs.

Discussion

To ascertain the cellular and molecular mechanism of vascular morphogenesis, we deleted FAK specifically in ECs. This genetic alteration leads to vascular deterioration and embryonic lethality before e11.5. Mutant ECs exhibited reduced cell spreading and survival, aberrant (but not reduced) migration, and no reduction in proliferation. This work demonstrates that FAK plays a cell-autonomous function in ECs that is essential

for vascular formation and maintenance, delineating cell survival as a major EC effect of FAK in vivo.

FAK as an intracellular transducer of angiogenic signaling

The role of FAK in transmitting angiogenic signals in ECs has been suggested through in vitro experiments (Orr and Murphy-Ullrich, 2004). Studies using *fak* knockouts also show that *fak* is required for angiogenesis in vivo (Ilic et al., 1995, 2003). However, because complete ablation deletes the *fak* gene in all cells, the precise function of FAK in ECs in vivo remains unknown. Furthermore, because *fak*-null embryos are defective in major developmental processes and die at e8.5, it is uncertain whether the vascular effect of FAK is secondary to the influence of other cell types and organs. We selectively targeted *fak* using the Tie2-Cre mice that we generated. Cre-mediated efficient recombination occurred in vascular progenitor cells at e7.5, and FAK was deleted in ~90% of ECs by e9.5. Specific vascular defects developed at e9.5, and 100% lethality occurred by e11.5. In addition, we identified similar defects in embryonic explants, suggesting that the vascular abnormalities are not secondary to other organ failure. Therefore, we conclude that FAK in ECs plays an essential role in early vascular development.

During the revision of this manuscript, Shen et al. (2005) reported that FAK in ECs is required for late, but not early, embryogenesis. Different Tie2-Cre mouse strains that were used are likely derived from different integration sites, and the onset of Cre activity could be different. Shen et al. (2005) demonstrated FAK deletion at e9.5, but it is unknown what fraction of ECs lost FAK. If the Tie2-Cre in the Shen et al. (2005) study was less efficient in early development, it could explain their late embryonic phenotype. Different floxed *fak* alleles were used as well. Our floxed allele targets the second kinase exon, as in the previously published *fak*-null allele (Ilic et al., 1995). Shen et al. (2005) used a floxed allele targeting the third exon. They demonstrated that their null allele resulted in a similar early lethality; thus, the temporal differences in the phenotype likely result from differences in Cre efficiency, and endothelial FAK is required for early vascular morphogenesis.

It is well recognized that proper formation of vascular trees involves vascular pruning to remove unnecessary vascular channels (Risau, 1997). Little is known about the cellular and molecular mechanisms involved in vascular regression. We identify a previously unappreciated molecular mechanism mediated by FAK signaling in the maintenance of vascular networks. Major vessels were established and well formed at e9.5, but by e10.5, virtually all of the major vessels had deteriorated in the mutants. This could have been a result of the general health of the embryos. However, time-lapse microscopy unequivocally revealed vessel regression in embryonic explants, supporting the notion that *fak* provides survival and stabilizing signals to ECs, thereby sustaining vascular integrity.

Cell survival is a major function of FAK in ECs

Based on cell culture experiments, it has been proposed that FAK regulates multiple effects in ECs, including cell migra-

tion, proliferation, and survival (Orr and Murphy-Ullrich, 2004; Shen et al., 2005). Reports from the complete knockout suggest that the loss of *fak* compromises migration and, thereby, impairs angiogenesis (Ilic et al., 1995, 2003). The precise cellular function of *fak* in ECs during angiogenesis in vivo remains to be elucidated. We took a conditional knockout approach combined with real-time imaging of angiogenic processes, demonstrating cell survival as a profound effect of FAK in ECs in vivo. No increase in apoptosis was found in $fak^{-/-}$ embryos (Ilic et al., 2003). The likely discrepancy is the detection sensitivity in the complete knockouts that die before e8.5. We counted 10,175 control and 7,878 mutant YS ECs and found increased TUNEL$^+$ ECs in mutants in vivo. We also investigated cell death by time-lapse microscopy and found an increase in EC death both at the sprout tips and in the existing network. Thus, our data show that loss of FAK can compromise cell survival, which could contribute to the vascular deterioration seen in the mutant embryos.

Multiple signaling molecules have been shown to function in EC survival. Vascular endothelial cadherin abolishes the survival signal from VEGF-A to Akt and Bcl2 (Carmeliet et al., 1999). Raf kinase mediates survival signals in ECs from basic fibroblast growth factor and VEGF (Alavi et al., 2003). RhoB controls Akt trafficking and regulates EC survival in vascular development (Adini et al., 2003). Our work demonstrates that FAK is a signaling mediator for EC survival, suggesting that it may be involved in one or more of these signaling pathways.

Cell proliferation is not significantly reduced in FAK-deficient ECs

It has been previously reported that FAK can promote cell proliferation in ECs and other cell types in vitro (Gilmore and Romer, 1996; Zhao et al., 1998). Thus, it is presumed that losing FAK would result in the reduction of cell proliferation. Shen et al. (2005) also demonstrated significant reduction in cell proliferation in cultured ECs, in which FAK was deleted in vitro. However, neither our in vivo BrdU and CD31 double staining nor the time-lapse microcopy on ECs in explants demonstrated a significant reduction in cell proliferation in mutants. Our results are consistent with other FAK knockout studies in which no significant change in proliferation was detected in vivo (Beggs et al., 2003; Ilic et al., 1995, 2003). Thus, our in vivo assay and organ cultures, which are more physiologically relevant, do not support a major function for FAK in EC proliferation in vivo.

FAK-deficient ECs exhibit a defective but not reduced motility

FAK-null fibroblasts derived from $fak^{-/-}$ embryos exhibit reduced cell motility (Ilic et al., 1995; Schlaepfer et al., 1999). However, Yano et al. (2004) reported that HeLa cells expressing reduced FAK by short inhibitory RNA and FAK-null fibroblasts exhibit increased cell motility. Thus, FAK's role in cell migration remains controversial. By time-lapse microscopy, we found that migration of FAK-deficient ECs lining the capillaries of the explants were indistinguishable from that of the controls. FAK-deficient ECs scattered outside of capillaries in

the explants, and single ECs grown on FN-coated dishes migrated faster than controls, although they did so unstably and lacked direction. FAK-deficient fibroblasts also show similar unstable, random migration (Wang et al., 2001a). Shen et al. (2005) reported reduced cell migration in response to FN in wound closure but not in the Boyden chamber assays. However, both assays can be influenced by cell proliferation and death, and because their ECs exhibit reduced proliferation and increased apoptosis, the migration defect required further validation. We believe that the organ cultures used in our studies are more physiologically relevant and that time-lapse microscopy can assess cell migration without influence from cell proliferation and death.

Our results raise alternative possibilities regarding FAK's motility function and present a conceptual advance beyond the idea that losing FAK results in reduced cellular motility and, thereby, compromises angiogenesis. Interestingly, WAVE2, a protein related to Wiskott-Aldrich syndrome, is critical for endothelial motility and seems to have a similar but distinct function to that of FAK. WAVE2$^{-/-}$ embryos also die around e10.5 with vascular defects. Reduced vessel size and enlarged intervessel areas were also evident, indicating typical sprouting angiogenic defects. Unlike the FAK mutants, WAVE2 mutant P-Sp explants failed to grow a vascular network, further suggesting that sprouting angiogenesis was impaired, possibly because of impaired cell migration (Yamazaki et al., 2003). Growth via sprouting, albeit reduced, occurs in the FAK mutant. Therefore, the loss of FAK may not completely impair EC migration in vivo. It is fascinating that there is differential motility in FAK-deficient ECs within or outside of a vascular structure, suggesting that FAK might differentially regulate EC migration in distinct angiogenic processes.

FAK-deficient ECs display defective lamellipodia and cell spreading

Changes in cell morphology after FAK depletion are crucial in understanding FAK's cellular function. We have demonstrated that FAK-deficient ECs spread poorly and lack cell polarity and round, broad lamellipodia, extending multiple pointing protrusions instead. The actin cytoskeleton was disorganized and contained reduced numbers, possibly aggregations, of focal adhesions. These morphological characteristics are consistent with the defects seen in primary mouse embryonic fibroblasts and cell lines expressing reduced levels of FAK (Yano et al., 2004). The fact that FAK is transiently localized to lamellipodia and membrane ruffles (Hsia et al., 2003) further supports the notion that it is important for these cellular structures. The cellular defects also provide a morphological explanation for the increase in cell death in these cells, as cell spreading is crucial for the survival of adherent cells (Frisch and Screaton, 2001). Compromised cytoskeletal organization could likely be the reason for their defective adhesion to substrata and spreading, which may explain the contraction seen in the explants. Together, the morphological defects exhibited in the FAK-deficient ECs are consistent with the defective cell behaviors resulting in vascular defects.

Mutant EC defects resembled those observed in cells with abnormal Rho family kinase signaling (Hall, 1998). The retractile behavior may result from increased Rho activity, whereas the aberrant lamellipodial protrusion may be caused by decreased Rac activity. Staining of phosphomyosin light chain, a major target of Rho kinase, revealed no gross alteration between the mutant and control ECs (unpublished data), suggesting that Rho activity may not be affected. Our current hypothesis is that Rac is a likely target of FAK in ECs, which is consistent with findings in FAK-null fibroblasts (Tilghman et al. 2005). However, the minimal number of ECs obtained from e9.5 embryos precludes Western blot analyses to test this hypothesis rigorously at the present time.

In summary, our finding that FAK is crucial for vascular stability during vascular development suggests FAK's role in diseased neovascularization, such as cancer and retinopathy, during which blood vessel growth contributes to both the pathogenesis and treatment of the diseases. It is conceivable that FAK might prove to be a promising target for anti-angiogenic therapy because deleting FAK can result in vascular regression.

Materials and methods

Mice
Generation of the *Tie2-Cre* transgenic (Tg) mice followed a previously described procedure (Wang et al., 2001b). Founder mice were identified by PCR genotyping, and the line was maintained in an FVB/N background. We crossed our *Tie2-Cre* mice with the *fak^{flox/flox}* and *fak^{+/-}* mice, which were maintained in a mixed background and genotyped as described previously (Beggs et al., 2003; Ilic et al., 1995). The *Tie1-GFP* mice have been previously described (Iljin et al., 2002). All animals were treated in accordance with the guidelines of the University of California San Francisco (UCSF) Institutional Animal Care and Use Committee.

Whole-mount LacZ and AP staining
LacZ staining was performed as previously described (Carlson et al., 2005; Carpenter et al., 2005). For AP staining, samples were fixed in 4% PFA overnight (o/n) and stained with BM purple according to the manufacturer's instructions (Roche).

Abs
Rat anti–mouse CD31, mouse anti-Pyk2, and mouse anti-Y397 phospho-FAK were obtained from BD Biosciences. Rabbit anti-FAK was purchased from Upstate Biotechnology. All secondary Abs were obtained from Jackson ImmunoResearch Laboratories. Cy3-conjugated mouse anti–mouse SMαA and rabbit anti-FN were purchased from Sigma Aldrich. Mouse anti-BrdU was obtained from the Developmental Studies Hybridoma Bank. Mouse anti–mouse paxillin was obtained from Zymed Laboratories, and AlexaFluor488-conjugated phalloidin was purchased from Invitrogen.

Cell isolation
Embryos and/or YSs from e8.5–10.5 were isolated into ice-cold PBS containing 1% FBS and 100 μg/ml penicillin and streptomycin and were treated with 200 U/ml collagenase III (Worthington Biochemical Corp.) in PBS for 15 min at 37°C. 10 μg/ml DNaseI (Sigma Aldrich) was added for the last 5 min. Cells were pelleted and plated on plates or glass coverslips coated with 10 μg/ml FN or 5 μg/ml LM for 12 h at 4°C or 0.1 mg/ml of 300-kD PLL hydrobromide for 5 min at RT and blocked with 0.2% BSA for 30 min. To purify ECs, cell pellets were resuspended in buffer with 2 μg/ml CD31 and incubated for 30 min followed by binding to Dynabeads M450 (Dynal) for an additional 30 min at 4°C with rocking. Cells were washed with buffer (0.1% BSA and 2 mM EDTA in PBS lacking Ca^{2+}/Mg^{2+}, pH 7.4). ECs were separated using a magnet and were plated on plates coated with 10 μg/ml FN. Cells were cultured in F-12 medium supplemented with 15% FBS, 0.1 μg/ml EC growth supplement (Collaborative Biomedical Products), and 100 μg/ml penicillin and streptomycin. Hematopoietic cells were dissociated by gentle mechanical disruption of e9.5 YSs, passed through a 45-μm strainer, and counted.

EC spreading and migration analysis

ECs isolated from e9.5 YSs were identified after a 1–3-h incubation with 2.5 μg/ml DiI-Ac-LDL (Biomedical Technologies). Cells were viewed with a time-lapse imaging system (Intelligent Imaging Innovations). ECs were maintained in a humidified 5% CO_2 mixture at 37°C. EC migration time-lapse recording frames were taken every 5–10 min continuously for up to 24 h.

Immunofluorescent staining of whole-mount specimens

Tissues were fixed in 4% PFA o/n, washed in PBS, and incubated in blocking solution (2% BSA plus 0.1% Triton X-100 in PBS) with primary Abs in blocking solution. After washing with blocking solution, they were incubated with the secondary Ab in blocking solution. All incubations were at 4°C for 12 h with gentle rocking.

Morphometric analysis of capillary beds

Five mutant and five littermate whole-mount control YSs were stained for CD31. Capillary images were taken in areas devoid of large vessels. 50 capillary diameters and intercapillary spaces were measured for each sample. 12 control and 4 mutant P-Sp explants were analyzed using the entire explant area after CD31 staining. Measurements were made with the ruler and pencil tools of Slidebook software (Intelligent Imaging Innovations). Diameters were measured from edge to edge at the point in the vessel located equidistant from its adjacent branches.

Histology and immunohistochemistry

Histology and immunohistochemistry were performed as previously described (Carpenter et al., 2005) using the Abs listed above.

Immunofluorescent staining of sections and isolated cells

Rehydrated paraffin sections were blocked with 5% donkey serum in PBS for 2 h at RT and incubated with the primary Ab at 4°C o/n followed by secondary Ab incubation for 1 h at 4°C. After being washed with PBS, samples were mounted with Vectashield containing DAPI (Vector Laboratories). Cells grown on coverslips were fixed in 4% PFA/PBS for 20 min and permeabilized in 0.1% Triton X-100/PBS for 3–10 min at RT before blocking in 1% BSA for 1 h, after which the same staining procedure was used.

Cell proliferation and TUNEL assays

BrdU labeling was performed using a kit from Zymed Laboratories. BrdU at 100 μg/g body weight was injected (i.v.) into pregnant females at gestation day 9.5 1 h before embryo collection. Cells were isolated as described above and cultured for 3 h. BrdU was detected according to the manufacturer's instructions.

To examine apoptotic ECs, e9.5 YSs were fixed in 4% PFA o/n, embedded in optimal cutting temperature, and frozen sectioned at 8 or 10 μm. Apoptosis of ECs was detected by double immunofluorescent staining for CD31 and subsequent TUNEL using a Fluorescein In Situ Apoptosis Detection Kit (Intergen Company). CD31^{+} ECs were counted, and the ratios of TUNEL^{+} CD31^{+} to total CD31^{+} ECs were obtained. Statistical analysis was performed using the t test.

Allantoic and P-Sp explants

Allantoic explants were cultured according to a previously published protocol (Downs et al., 1998) except that 50% FCS was used instead of 50% rat serum. Allantoises were isolated at the four to six–somite stage and cultured for 54 h on FN-coated dishes. Explants were stained with anti-CD31 as described in Immunofluorescent staining of sections and isolated cells.

For P-Sp explants, the P-Sp region of an embryo was dissected and placed into a 12-well dish on top of a confluent OP9 stromal cell layer according to methods described previously (Takakura et al., 1998). Explants were cultured in RPMI 1640 medium supplemented with 10% FBS, which was changed daily. *Tie1-GFP* Tg ECs were imaged as described above (in EC spreading and migration analysis) every 5–10 min for up to 5 d. For EC migration analyses, the XY coordinates of single ECs and capillary ECs were tracked.

Western blotting and IP

Western blotting and IP was performed as previously described (Wang et al. 2001b) using a polyclonal anti-FAK Ab or a polyclonal anti-Pyk2 Ab. IP was performed to detect FRNK using a monoclonal anti-FAK Ab (clone 2A7) that targets the COOH terminus of FAK and FRNK.

Online supplemental material

EC and capillary structure dynamics were monitored in *Tie1-GFP* Tg control (Video 1) and mutant (Video 2) P-Sp explants. Chemokinetics of isolated e9.5 control (Video 3) and mutant (Video 4) YS ECs 18 h after plating on FN is also shown. There was no obvious induction of Pyk2 expression in FAK-null ECs (Fig. S1). Online supplemental material is available at http://www.jcb.org/cgi/content/full/jcb.200506184/DC1.

References

Abu-Ghazaleh, R., J. Kabir, H. Jia, M. Lobo, and I. Zachary. 2001. Src mediates stimulation by vascular endothelial growth factor of the phosphorylation of focal adhesion kinase at tyrosine 861, and migration and anti-apoptosis in endothelial cells. *Biochem. J.* 360:255–264.

Adini, I., I. Rabinovitz, J.F. Sun, G.C. Prendergast, and L.E. Benjamin. 2003. RhoB controls Akt trafficking and stage-specific survival of endothelial cells during vascular development. *Genes Dev.* 17:2721–2732.

Alavi, A., J.D. Hood, R. Frausto, D.G. Stupack, and D.A. Cheresh. 2003. Role of Raf in vascular protection from distinct apoptotic stimuli. *Science.* 301:94–96.

Ausprunk, D.H., and J. Folkman. 1977. Migration and proliferation of endothelial cells in preformed and newly formed blood vessels during tumor angiogenesis. *Microvasc. Res.* 14:53–65.

Beggs, H.E., D. Schahin-Reed, K. Zang, S. Goebbels, K.A. Nave, J. Gorski, K.R. Jones, D. Sretavan, and L.F. Reichardt. 2003. FAK deficiency in cells contributing to the basal lamina results in cortical abnormalities resembling congenital muscular dystrophies. *Neuron.* 40:501–514.

Burri, P.H., and V. Djonov. 2002. Intussusceptive angiogenesis–the alternative to capillary sprouting. *Mol. Aspects Med.* 23:S1–S27.

Carlson, T.R., Y. Yan, X. Wu, M.T. Lam, G.L. Tang, L.J. Beverly, L.M. Messina, A.J. Capobianco, Z. Werb, and R. Wang. 2005. Endothelial expression of constitutively active Notch4 elicits reversible arteriovenous malformations in adult mice. *Proc. Natl. Acad. Sci. USA.* 102:9884–9889.

Carmeliet, P. 2003. Angiogenesis in health and disease. *Nat. Med.* 9:653–660.

Carmeliet, P., M.G. Lampugnani, L. Moons, F. Breviario, V. Compernolle, F. Bono, G. Balconi, R. Spagnuolo, B. Oostuyse, M. Dewerchin, et al. 1999. Targeted deficiency or cytosolic truncation of the VE-cadherin gene in mice impairs VEGF-mediated endothelial survival and angiogenesis. *Cell.* 98:147–157.

Carpenter, B., Y. Lin, S. Stoll, R.L. Raffai, R. McCuskey, and R. Wang. 2005. VEGF is crucial for the hepatic vascular development required for lipoprotein uptake. *Development.* 132:3293–3303

Downs, K.M., S. Gifford, M. Blahnik, and R.L. Gardner. 1998. Vascularization in the murine allantois occurs by vasculogenesis without accompanying erythropoiesis. *Development.* 125:4507–4520.

Frisch, S.M., and R.A. Screaton. 2001. Anoikis mechanisms. *Curr. Opin. Cell Biol.* 13:555–562.

Gilmore, A.P., and L.H. Romer. 1996. Inhibition of focal adhesion kinase (FAK) signaling in focal adhesions decreases cell motility and proliferation. *Mol. Biol. Cell.* 7:1209–1224.

Haar, J.L., and G.A. Ackerman. 1971. A phase and electron microscopic study of vasculogenesis and erythropoiesis in the yolk sac of the mouse. *Anat. Rec.* 170:199–223.

Hall, A. 1998. Rho GTPases and the actin cytoskeleton. *Science.* 279:509–514.

Hsia, D.A., S.K. Mitra, C.R. Hauck, D.N. Streblow, J.A. Nelson, D. Ilic, S. Huang, E. Li, G.R. Nemerow, J. Leng, et al. 2003. Differential regulation of cell motility and invasion by FAK. *J. Cell Biol.* 160:753–767.

Ilic, D., Y. Furuta, S. Kanazawa, N. Takeda, K. Sobue, N. Nakatsuji, S. Nomura, J. Fujimoto, M. Okada, and T. Yamamoto. 1995. Reduced cell motility and enhanced focal adhesion contact formation in cells from FAK-deficient mice. *Nature.* 377:539–544.

Ilic, D., B. Kovacic, S. McDonagh, F. Jin, C. Baumbusch, D.G. Gardner, and C.H. Damsky. 2003. Focal adhesion kinase is required for blood vessel morphogenesis. *Circ. Res.* 92:300–307.

Iljin, K., T.V. Petrova, T. Veikkola, V. Kumar, M. Poutanen, and K. Alitalo. 2002. A fluorescent Tie1 reporter allows monitoring of vascular development and endothelial cell isolation from transgenic mouse embryos. *FASEB J.* 16:1764–1774.

Kim, I., S.O. Moon, S.K. Park, S.W. Chae, and G.Y. Koh. 2001. Angiopoietin-1 reduces VEGF-stimulated leukocyte adhesion to endothelial cells by reducing ICAM-1, VCAM-1, and E-selectin expression. *Circ. Res.* 89:477–479.

Kurz, H., T. Gartner, P.S. Eggli, and B. Christ. 1996. First blood vessels in the avian neural tube are formed by a combination of dorsal angioblast immigration and ventral sprouting of endothelial cells. *Dev. Biol.* 173:133–147.

Lobe, C.G., K.E. Koop, W. Kreppner, H. Lomeli, M. Gertsenstein, and A. Nagy. 1999. Z/AP, a double reporter for cre-mediated recombination. *Dev. Biol.* 208:281–292.

Mao, X., Y. Fujiwara, and S.H. Orkin. 1999. Improved reporter strain for monitoring Cre recombinase-mediated DNA excisions in mice. *Proc. Natl. Acad. Sci. USA.* 96:5037–5042.

Maru, Y., S.K. Hanks, and M. Shibuya. 2001. The tubulogenic activity associated with an activated form of Flt-1 kinase is dependent on focal adhesion kinase. *Biochim. Biophys. Acta.* 1540:147–153.

Miranti, C.K., and J.S. Brugge. 2002. Sensing the environment: a historical perspective on integrin signal transduction. *Nat. Cell Biol.* 4:E83–E90.

Moore, K., and T. Persaud. 2003. The Developing Human: Clinically Oriented Embryology. W.B. Saunders Co., Philadelphia. 575 pp.

Newman, P.J., M.C. Berndt, J. Gorski, G.C. White II, S. Lyman, C. Paddock, and W.A. Muller. 1990. PECAM-1 (CD31) cloning and relation to adhesion molecules of the immunoglobulin gene superfamily. *Science.* 247:1219–1222.

Orr, A.W., and J.E. Murphy-Ullrich. 2004. Regulation of endothelial cell function BY FAK and PYK2. *Front. Biosci.* 9:1254–1266.

Parsons, J.T. 2003. Focal adhesion kinase: the first ten years. *J. Cell Sci.* 116:1409–1416.

Polte, T.R., A.J. Naftilan, and S.K. Hanks. 1994. Focal adhesion kinase is abundant in developing blood vessels and elevation of its phosphotyrosine content in vascular smooth muscle cells is a rapid response to angiotensin II. *J. Cell. Biochem.* 55:106–119.

Qi, J.H., and L. Claesson-Welsh. 2001. VEGF-induced activation of phosphoinositide 3-kinase is dependent on focal adhesion kinase. *Exp. Cell Res.* 263:173–182.

Risau, W. 1997. Mechanisms of angiogenesis. *Nature.* 386:671–674.

Risau, W., and I. Flamme. 1995. Vasculogenesis. *Annu. Rev. Cell Dev. Biol.* 11:73–91.

Rossant, J., and L. Howard. 2002. Signaling pathways in vascular development. *Annu. Rev. Cell Dev. Biol.* 18:541–573.

Schlaeger, T.M., S. Bartunkova, J.A. Lawitts, G. Teichmann, W. Risau, U. Deutsch, and T.N. Sato. 1997. Uniform vascular-endothelial-cell-specific gene expression in both embryonic and adult transgenic mice. *Proc. Natl. Acad. Sci. USA.* 94:3058–3063.

Schlaepfer, D.D., C.R. Hauck, and D.J. Sieg. 1999. Signaling through focal adhesion kinase. *Prog. Biophys. Mol. Biol.* 71:435–478.

Schlaepfer, D.D., S.K. Mitra, and D. Ilic. 2004. Control of motile and invasive cell phenotypes by focal adhesion kinase. *Biochim. Biophys. Acta.* 1692:77–102.

Shen, T.L., A.Y. Park, A. Alcaraz, X. Peng, I. Jang, P. Koni, R.A. Flavell, H. Gu, and J.L. Guan. 2005. Conditional knockout of focal adhesion kinase in endothelial cells reveals its role in angiogenesis and vascular development in late embryogenesis. *J. Cell Biol.* 169:941–952.

Sieg, D.J., C.R. Hauck, D. Ilic, C.K. Klingbeil, E. Schaefer, C.H. Damsky, and D.D. Schlaepfer. 2000. FAK integrates growth-factor and integrin signals to promote cell migration. *Nat. Cell Biol.* 2:249–256.

Takakura, N., X.L. Huang, T. Naruse, I. Hamaguchi, D.J. Dumont, G.D. Yancopoulos, and T. Suda. 1998. Critical role of the TIE2 endothelial cell receptor in the development of definitive hematopoiesis. *Immunity.* 9:677–686.

Tilghman, R.W., J.K. Slack-Davis, N. Sergina, K.H. Martin, M. Iwanicki, E.D. Hershey, H.E. Beggs, L.F. Reichardt, and J.T. Parsons. 2005. Focal adhesion kinase is required for the spatial organization of the leading edge in migrating cells. *J. Cell Sci.* 118:2613–2623.

Wang, H.B., M. Dembo, S.K. Hanks, and Y. Wang. 2001a. Focal adhesion kinase is involved in mechanosensing during fibroblast migration. *Proc. Natl. Acad. Sci. USA.* 98:11295–11300.

Wang, R., L.D. Ferrell, S. Faouzi, J.J. Maher, and J.M. Bishop. 2001b. Activation of the Met receptor by cell attachment induces and sustains hepatocellular carcinomas in transgenic mice. *J. Cell Biol.* 153:1023–1034.

Yamazaki, D., S. Suetsugu, H. Miki, Y. Kataoka, S. Nishikawa, T. Fujiwara, N. Yoshida, and T. Takenawa. 2003. WAVE2 is required for directed cell migration and cardiovascular development. *Nature.* 424:452–456.

Yancopoulos, G.D., S. Davis, N.W. Gale, J.S. Rudge, S.J. Wiegand, and J. Holash. 2000. Vascular-specific growth factors and blood vessel formation. *Nature.* 407:242–248.

Yano, H., Y. Mazaki, K. Kurokawa, S.K. Hanks, M. Matsuda, and H. Sabe. 2004. Roles played by a subset of integrin signaling molecules in cadherin-based cell-cell adhesion. *J. Cell Biol.* 166:283–295.

Zhao, J.H., H. Reiske, and J.L. Guan. 1998. Regulation of the cell cycle by focal adhesion kinase. *J. Cell Biol.* 143:1997–2008.